Novel Use of an Osmolyte To Dissect Multiple Thermodynamic Linkages in a Chemokine Ligand−Receptor System[†]

Lavanya Rajagopalan, Jörg Rösgen, David Wayne Bolen, and Krishna Rajarathnam*

Department of Human Biological Chemistry and Genetics and Sealy Center for Structural Biology, The University of Texas Medical Branch, Galveston, Texas 77555-1055

Received June 24, 2005; Revised Manuscript Received August 5, 2005

ABSTRACT: We have used trimethylamine *N*-oxide (TMAO), a protecting osmolyte, to dissect the complex thermodynamic linkages involved in the interaction between the chemokine interleukin-8 (IL-8) and the N-domain of its receptor CXCR1. Our results show that TMAO induces folding in the CXCR1 receptor N-domain and that the N-domain upon folding binds ligand with higher affinity. This represents, to our knowledge, the smallest domain that has been shown to be folded in osmolyte. Using the phase diagram method to analyze this thermodynamic relationship graphically, we also observe that TMAO favors ligand dimerization and that the dimeric ligand binds the receptor domain with lower affinity. We have thus been able to dissect coupling among three distinct processes, receptor domain folding, ligand dimerization, and ligand−receptor domain binding in this chemokine−receptor system. We also observe that the affinity of the related chemokine, melanoma growth stimulatory activity (MGSA), increases concurrent with N-domain folding similar to IL-8 but shows more profound differences on ligand dimerization. These studies establish a novel and innovative use of osmolytes to dissect linkages among different processes and exploit the phase diagram as a tool to graphically represent and dissect complex thermodynamic relationships in biological systems. On the basis of our observations and earlier work, we discuss the relevance of ligand dimerization in chemokine regulation.

Osmolytes are small organic (co)solutes that play a prominent role in the biology of nearly all taxa (*1*). Such osmolytes are known to accumulate in archea as well as higher plants and animals including humans and modulate the behavior of biological macromolecules in vivo (*2*). Many of these solutes are found naturally in organisms living under harsh environmental stresses such as high temperature, salinity, and pressure and have evolved an exceptional ability to protect and promote the native states of proteins in the presence of such denaturing stresses (*2*). These solutes appear to have been naturally selected on the basis of their unfavorable interactions with the peptide backbone, a solvophobic effect that has been termed the "osmophobic effect" (*3*). By their unfavorable interactions with the protein backbone, these protecting osmolytes preferentially raise the free energy of the unfolded state and shift the equilibrium in favor of the folded state, thereby stabilizing the folded state of proteins (*3*). This ability of protecting osmolytes to force natively unfolded and partially disordered proteins to adopt definite conformations has proven to be a valuable tool in structural and functional characterization of such intrinsically disordered proteins and has also provided fundamental insights into the energetic coupling between folding and ligand binding (*4*−*7*). In this study, the osmolyte trimethylamine oxide (TMAO)[1] has been used to dissect a more complex linkage among three different processes: receptor domain folding, ligand binding, and dimerization in a chemokine−receptor system.

Chemokines, or *chemo*tactic cyto*kines*, are small soluble proteins that play fundamental regulatory roles in native immunity, in inflammation, and in developmental processes by binding and activating 7-transmembrane receptors that belong to the G-protein-coupled receptor (GPCR) class (*8*). A characteristic feature of chemokine ligands is their propensity to undergo monomer−dimer equilibrium under physiological conditions. Interleukin-8 (IL-8; also known as CXCL8), one of the best-studied members of the chemokine family, dimerizes at micromolar concentrations, and both NMR and X-ray structures show it to be a dimer (*9*, *10*). However, using trapped nonassociating monomers and studying binding to the receptor N-domain under conditions where both monomer and dimer exist, it has been shown that a monomer is sufficient and that dimer dissociation is essential for high-affinity receptor binding (*11*, *12*). These observations have further led to the hypothesis that ligand dimerization functions as a negative regulator for receptor function (*12*). IL-8 is a high-affinity ligand for the chemokine receptor CXCR1, while the related chemokine melanoma growth stimulatory activity (MGSA) binds CXCR1 with 50−100-fold lower affinity (*13*, *14*). Knowledge of the structural

[†] This work was supported by the American Heart Association Texas Affiliate Grant 0365112Y (to K.R.), by a McLaughlin Predoctoral Fellowship (to L.R.), and by a training fellowship from the W. M. Keck Foundation (to J.R.).

* To whom correspondence should be addressed. Tel: 409-772-2238. Fax: 409-772-1790. E-mail: krrajara@utmb.edu.

[1] Abbreviations: CXCR1, CXC chemokine receptor 1; IL-8, interleukin-8; MGSA, melanoma growth stimulatory activity; N-domain, N-terminal domain; K_d, dissociation constant; CD, circular dichroism; TMAO, trimethylamine *N*-oxide; Trp, tryptophan.

10.1021/bi051219z CCC: $30.25 © 2005 American Chemical Society
Published on Web 09/10/2005

and thermodynamic basis of the receptor affinities and selectivities of chemokines and their receptors is essential for understanding the function and regulation of these proteins in vivo.

Whereas the structure determination of soluble chemokine ligands has been straightforward, the size and hydrophobicity of these membrane-bound receptors are major roadblocks in obtaining this knowledge. The studies detailed here attempt to bridge this chasm by studying structural and functional characteristics of individual functional domains, such as the CXCR1 N-domain. This domain forms one of the two binding sites for ligand on the intact receptor, is structured in micelles that mimic the native membrane environment, and has been shown to be a major determinant of ligand-binding affinity (*15*). We have shown previously that differences in IL-8 and MGSA binding affinity do not arise from binding interactions at the N-domain in isolation but from thermodynamic coupling between the two sites of ligand−receptor interaction (*15*).

The receptor N-domain is unstructured in solution but adopts definite structure in its native membrane environment. In this study, TMAO, a protecting osmolyte, has been used to force-fold the chemokine receptor CXCR1 N-domain. We have investigated the effect of folding the N-domain on its binding affinity for two different ligands, IL-8 and MGSA. We observe nativelike binding affinities in the presence of TMAO, indicating the induction of nativelike structure and the presence of thermodynamic linkage between folding and binding. The phase diagram method has been used to represent the folding and binding data (*16*) and has provided insights into yet another process, ligand dimerization, that is thermodynamically linked to receptor domain folding and ligand binding. In addition, differences are also apparent between the interactions of IL-8 and MGSA with the CXCR1 N-domain, and the implications of the above findings are discussed.

EXPERIMENTAL PROCEDURES

Synthesis and Labeling of the CXCR1 N-Domain. The rabbit CXCR1 N-domain (34 amino acids) was synthesized by solid-phase peptide synthesis and purified as described previously (*15*). We also synthesized a scrambled N-domain peptide for use as a negative control. N-domain: LWTW-FEDEFANATGMPPVEKDYSPSLVVTQTLNK. Scrambled N-domain: DVPLSTSATEGKTAWDKQVMLFTLPNEY-FNVWPE. These peptides have been extensively characterized previously and have provided valuable information on the structural basis of IL-8 binding to the CXCR1 receptor (*12*, *15*). The peptides were labeled with AlexaFluor488, a fluorescein derivative, for the fluorescence experiments described below. AlexaFluor488 was obtained as a reactive succinimidyl ester from Molecular Probes, Inc. (Eugene, OR). The labeling reaction was carried out using 1.2 mg of the N-domain peptide and 1 mg of AlexaFluor488 in a 2 mL reaction volume in 20 mM HEPES buffer, pH 7.4. The reaction was allowed to proceed for 1 h at room temperature in the dark, and the labeled protein was purified by gel filtration on a Sephadex 30 column. The extent of labeling was determined by measuring absorbance at 280 and 488 nm, λ_{max} of the protein and probe, respectively. The presence of homogeneously labeled protein was also confirmed using MALDI time-of-flight mass spectrometry. The scrambled peptide was also labeled with AlexaFluor488 in a similar manner.

Expression, Synthesis, and Purification of IL-8, MGSA, and "Trapped" IL-8 Variants. Wild-type human IL-8 and MGSA were bacterially expressed and purified as described previously (*15*). The trapped nonassociating monomeric IL-8 (L25NMe IL-8) was chemically synthesized and contains a methyl group substitution for the backbone amide proton for Leu25. This substitution, in addition to breaking two H-bonds about the 2-fold symmetry, introduces steric bulk at the dimer interface, and this monomeric variant has been shown to have native activity (*11*, *17*). The trapped nondissociating dimer IL-8 (R26C) was also chemically synthesized and involved introducing a Cys substitution for Arg at the 2-fold symmetry. NMR studies have shown that introduction of the disulfide at the dimer interface does not perturb the structure, and the structure of the R26C mutant is essentially identical to the native dimer. Further, compared to the monomer, this variant shows significantly lower binding to the receptor (unpublished observations). Both of these variants were synthesized at the Biomedical Research Centre, Vancouver, Canada.

Fluorescence Studies. (A) Folding Studies. All fluorescence spectra were measured on a Spex Fluoromax fluorometer at 23 °C in 50 mM Tris and 50 mM sodium chloride, pH 8.0, buffer. For tryptophan fluorescence (Trp), spectra were measured from 300 to 400 nm with excitation at 280 nm, and for Alexa fluorescence, spectra were measured from 485 to 550 nm with excitation at 465 nm. Folding studies were carried out by measuring Alexa fluorescence of individual samples containing a fixed amount of receptor peptide and increasing TMAO concentrations from 0 to 4 M. The fluorescence intensity at 519 nm (the emission maximum of conjugated AlexaFluor488) was normalized and plotted against TMAO concentration to obtain a folding curve and fitted using the linear extrapolation method (*18*).

(B) Ligand-Binding Studies. Ligand-binding studies were carried out in 50 mM Tris and 50 mM sodium chloride, pH 8.0, buffer containing different fixed concentrations of TMAO. Receptor peptide was used at a fixed concentration of 0.2−0.5 μM, with increasing concentrations of either IL-8 or MGSA. Fluorescence emissions of the blank IL-8, MGSA, and TMAO solutions were found to be negligible at the wavelengths used, so blank subtractions were deemed unnecessary. The fluorescence intensity at 519 nm was normalized and plotted against ligand concentration to obtain binding curves. All curves were normalized using SigmaPlot 8.0 software and fitted to a simple one-site binding equation using the nonlinear least-squares fitting algorithm from Origin software, taking into account the amount of bound vs free ligand. We used a scrambled peptide and observed no change in Alexa fluorescence indicating no binding and that ligand binding to the native receptor N-domain is specific (data not shown).

Circular Dichroism (CD) Studies. All CD spectra were collected on an AVIV 62DS CD spectrometer at 25 °C in 50 mM sodium phosphate and 50 mM sodium chloride, pH 8.0, buffer with increasing TMAO concentration. Spectra were recorded from 190 to 250 nm as an average of three scans and smoothed to obtain the final data. The ellipticity at 222 nm was normalized and plotted against TMAO

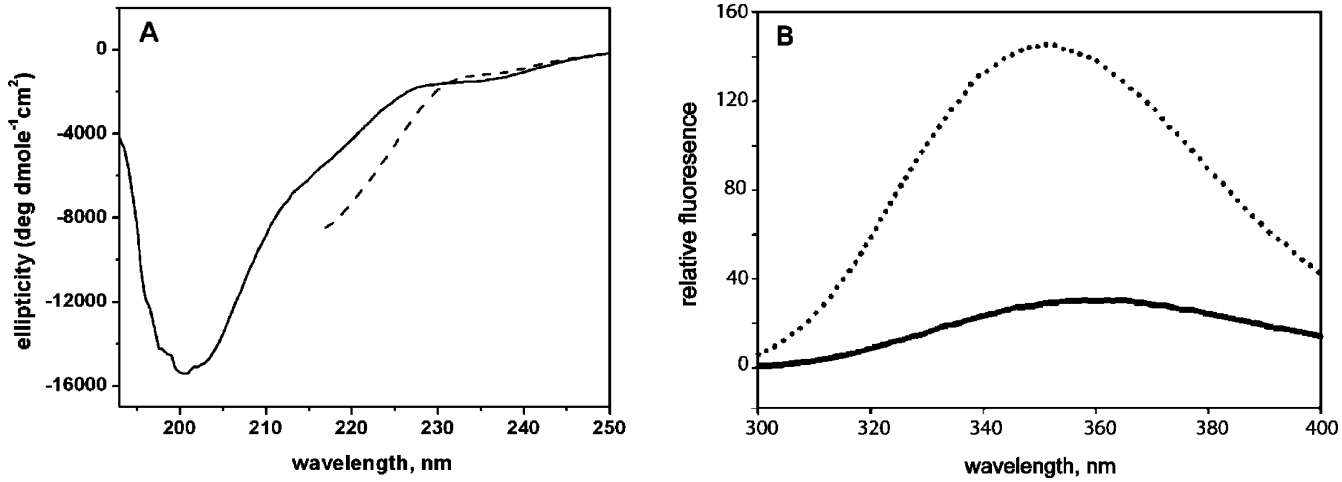

FIGURE 1: CD (A) and tryptophan fluorescence (B) spectra of the CXCR1 N-domain in TMAO. The minimum at 222 nm in the CD spectrum and increased tryptophan fluorescence and a blue shift are evidence of structure in TMAO. The spectra were measured in 50 mM sodium phosphate and 50 mM sodium chloride buffer (pH 8.0) with (—) or without (- - -) 2 M TMAO.

concentration to obtain a folding curve. Due to the inherent noise in CD spectra, the data could not be fitted using the linear extrapolation method but were superimposable on the fit to the fluorescence data.

RESULTS AND DISCUSSION

Folding of the CXCR1 N-Domain. The CD and Trp fluorescence spectra indicate that the N-domain, which is unstructured in solution, adopts a defined conformation in TMAO (Figure 1). However, we could not reliably measure Trp fluorescence intensity at higher TMAO concentrations. The Alexa probe showed stable fluorescence in TMAO and, in addition, proved to be a sensitive probe of folding and ligand binding, and so we have used the AlexaFluor488-labeled receptor domain for all further experiments. Such a tag also allows IL-8 binding measurements straightforwardly, with no interference from the single Trp residue in the IL-8 sequence. Further, we observed no change in fluorescence of the AlexaFluor488-labeled scrambled peptide in TMAO, indicating that the scrambled peptide does not fold and also that Alexa fluorescence is not influenced by TMAO in the absence of folding (data not shown).

The folding monitored using Alexa fluorescence as a probe yields a folding transition with a free energy change of −1.7 kcal/mol and a transition midpoint ($c_{1/2}$) at 1.6 M TMAO (Figure 2). Folding isotherms obtained from fluorescence and CD data are superimposable, confirming that the folding transition is two state (data not shown). This represents, to our knowledge, the smallest protein domain (34 amino acids) that is folded by an osmolyte. We have previously shown that the N-domain adopts a defined conformation in detergent micelles that mimic the membrane environment (*15*). The ability of the CXCR1 N-domain to fold in the presence of osmolyte shows that the isolated receptor N-domain has an innate propensity to be structured and functions as an independent functional unit in the intact receptor.

Dependence of Ligand-Binding Affinity upon the Folded State. We investigated the effect of TMAO-induced structure of the receptor N-domain on ligand-binding affinity. Ligand-binding studies show that the affinity of the N-domain for IL-8 is progressively higher in the presence of increasing TMAO concentrations (Table 1, Figure 3). The ability of

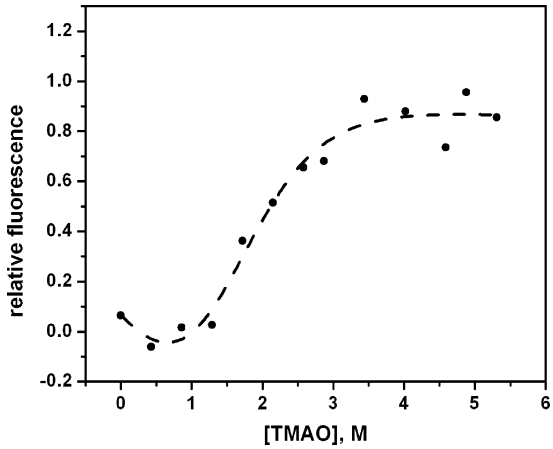

FIGURE 2: Folding of the CXCR1 N-domain as a function of TMAO concentration, monitored using Alexa fluorescence. The ΔG of folding is -1.7 ± 0.2 kcal/mol, and the folding midpoint ($c_{1/2}$) is at 1.6 M TMAO. The fluorescence measurements were carried out with excitation at 465 nm and emission at 519 nm in 50 mM Tris and 50 mM sodium chloride buffer, pH 8.0.

Table 1: Ligand-Binding Affinities of the CXCR1 N-Domain

ligand	[TMAO] (M)	K_d (μM)
WT IL-8	0	3 ± 0.3
WT IL-8	1	1 ± 0.3
WT IL-8	2.1	0.6 ± 0.06
WT IL-8	3.2	0.6 ± 0.12
L25NMe IL-8[b]	0	2.8 ± 0.4
L25NMe IL-8[b]	3	0.2 ± 0.07
R26C IL-8[c]	0	ND[a]
R26C IL-8[c]	3	ND[a]
WT MGSA	0	ND[a]
WT MGSA	0.8	7.4 ± 0.7
WT MGSA	1.7	1.6 ± 0.7
WT MGSA	2.5	ND[a]
WT MGSA	3.2	ND[a]

[a] ND: not detected. [b] L25NMe IL-8: trapped monomeric IL-8. [c] R26C IL-8: trapped dimeric IL-8.

osmolyte to induce progressive gain of function in the N-domain indicates that TMAO-induced folding is functionally significant; i.e., folding of the CXCR1 receptor N-domain is thermodynamically coupled to ligand binding. This thermodynamic linkage can be dissected rigorously using TMAO, as the ligand-binding affinity of the N-domain at

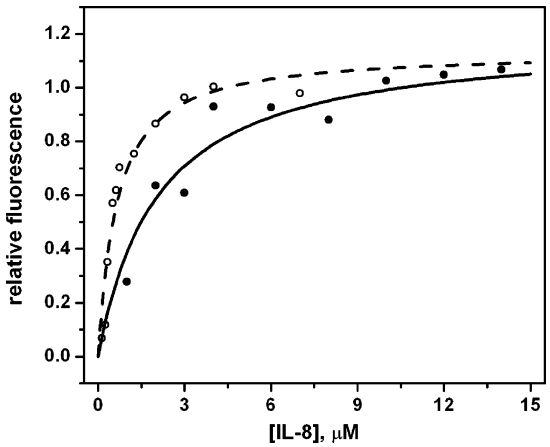

FIGURE 3: Binding of the CXCR1 N-domain to IL-8 in TMAO. The affinity for IL-8 is significantly higher in TMAO (○) than in solution (●). The fluorescence measurements were carried out with excitation at 465 nm and emission at 519 nm in 50 mM Tris and 50 mM sodium chloride, pH 8.0, with or without 3 M TMAO.

Table 2: Folding Midpoint Values of the CXCR1 N-Domain

[IL-8] (μM)	TMAO folding midpoint (M)
0	1.6 ± 0.3
0.1	1.4 ± 0.2
0.3	1.3 ± 0.2

different population ratios of folded/unfolded molecules can be quantitated at different TMAO concentrations.

To further understand the linkage between receptor domain folding and ligand binding, we carried out folding studies in the presence of low IL-8 concentrations (0.1−0.3 μM). The presence of thermodynamic linkage between the processes of N-domain folding and ligand binding would indicate that each process influences the other; therefore, binding of ligand to the N-domain should influence its ability to fold in osmolyte. We observed that the folding isotherm is shifted to the left in the presence of increasing IL-8 concentrations. In other words, the midpoint of the folding transition shifts toward lower TMAO concentrations in the presence of IL-8 (Table 2). This reiterates the presence of positive thermodynamic linkage between receptor N-domain folding and ligand binding. Notwithstanding intrinsic error in these measurements, the trend toward lower TMAO concentrations is noticeable (Table 2). These results along with the ligand-binding affinities from Table 1 provide a fairly conclusive picture of the coupling between folding and binding, as is evident from analysis of the data using the phase diagram as described below.

Analysis of Thermodynamic Linkages Using the Phase Diagram Approach. The combined results from binding and folding experiments can be summarized graphically in a phase diagram (Figure 4). This method facilitates the quantitative interpretation of stoichiometries and positive/negative linkages in ligand binding (*16*). Unlike conventional representation of linkage schemes such as shown in Scheme 1, the phase diagram affords a visual depiction of linkage relations and is hence more intuitively interpretable.

In a reaction scheme that involves protein unfolding and ligand binding to the native state, the relative partition function is given by (*16*)

$$Q = Q_F + Q_U + Q_{FL} = 1 + K + K_B[L] \qquad (1)$$

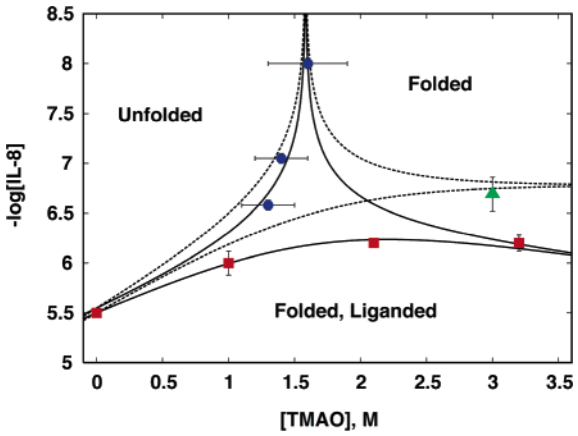

FIGURE 4: Phase diagram showing transitions between unfolded, folded, and folded/liganded states of the CXCR1 N-domain. The lines represent 50% populations of each state. Solid lines indicate the fit of actual data taken from Tables 1 and 2. The data points represent the pK_d values of IL-8 binding at different TMAO concentrations (red boxes) and midpoints of the folding transition at different IL-8 concentrations (blue circles). Error bars shown represent standard deviations from the mean of three or more experiments (data shown in Tables 1 and 2). Resulting fit parameters for eqs 2−6: log K and log K_B at 0 M TMAO = 1.255 and 6.778, m = 4.6 kJ/(mol·M), and m_B = 1.1 kJ/(mol·M). Predicted transition lines in the absence of dimerization (m_B = 0) are shown (···). The experimentally determined binding affinity of L25NMe IL-8 (monomer) in 3 M TMAO is also shown (green triangle).

Scheme 1: Conventional Representation of Linkage

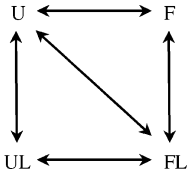

where K = [U]/[F] is the equilibrium constant of unfolding and K_B = [FL]/([F][L]) is the binding constant. On the phase separation line between the native and unfolded state, the unfolded state has the same population size as the sum of the other two states. Therefore, the following relation holds:

$$[L]_{50\%U} = (K - 1)/K_B \qquad (2)$$

Analogously, we have

$$[L]_{50\%FL} = (1 + K)/K_B \qquad (3)$$

and

$$[L]_{50\%F} = (1 - K)/K_B \qquad (4)$$

The equilibrium constant K depends on the osmolyte concentration c according to the linear extrapolation method (*18*):

$$\Delta G = -RT \log K = \Delta G(0\ M) + mc \qquad (5)$$

The binding constant K_B is defined the same way:

$$\Delta G_B = -RT \log K_B = \Delta G_B(0\ M) + m_B c \qquad (6)$$

The phase diagram (Figure 4) plots concentration of TMAO on the abscissa and IL-8 concentration (expressed as the negative logarithm) on the ordinate. The phase diagram is therefore a graphical representation of unfolded, folded,

and ligand-bound populations of the N-domain at different TMAO and IL-8 concentrations. The solid lines are phase separation lines indicating 50% population size or, in other words, the midpoint of the respective processes. For example, the line separating the "folded" and "unfolded" populations indicates the midpoint of the folding transition (i.e., the $c_{1/2}$) at each IL-8 concentration, while the line separating the "folded, liganded" population from the rest indicates the midpoints of ligand binding (i.e., the K_b) at each TMAO concentration. The solid lines are fits to the experimental data from Tables 1 and 2.

In such a concentration vs concentration phase diagram, the slopes of the 50% phase separation lines indicate the ratios of the stoichiometries or *m*-values of the respective interactions (*16*). According to the mechanism of osmolyte-induced folding, TMAO disfavors exposure of peptide groups. The *m*-value of folding can be said to roughly correlate with the number of peptide groups buried due to unfavorable interaction with osmolyte. Folding of the receptor domain would bury considerably more of the peptide backbone than ligand binding alone; therefore, the *m*-value would be higher at lower concentrations of TMAO (where folding and binding occur simultaneously) and lower at higher TMAO concentrations (where folding is complete and only binding occurs). This allows for the prediction of slopes in Figure 4. The dotted lines indicate the expected slopes of each phase separation line based on the observed stoichiometry of binding and the *m*-value of forced folding. At very low ligand concentrations (at the top of the phase diagram), the slope of the predicted phase separation line (the ratio of the folding *m*-value over ligand-binding stoichiometry) is infinite, indicating a stoichiometry of zero, i.e., the absence of significant ligand binding. At the lower left of the diagram (where folding and binding occur simultaneously), the phase separation line is predicted to have a large positive slope, indicating the large *m*-value of folding, as indicated by the predicted line. At the right of the phase diagram, the predicted slope is shallow, indicating that the *m*-value is lower at these high TMAO concentrations, where folding is complete and ligand binding is the predominant interaction.

From the experimental fit to the data (solid line), it is apparent that there is a positive dependency of binding affinity on TMAO concentration as expected, up to about ~2 M. At higher TMAO concentrations, however, there is a detectable *negative* slope, indicating a negative dependency of binding affinity on TMAO concentration. As discussed above, the slope of the phase separation line indicates the ratios of the stoichiometries or *m*-values of the represented interactions. If the phase diagram represents only two linked processes of N-domain folding and ligand binding, there are two possible explanations for this negative ratio between *m*-value of folding and binding stoichiometry. The first is that, at concentrations above 2 M, TMAO *disfavors* ligand binding, so that there is actually ligand dissociation from the N-domain, giving rise to a negative stoichiometry and therefore a negative slope. The other possibility is that, at higher TMAO concentrations, the *m*-value becomes negative; i.e., peptide groups become exposed rather than buried. Neither explanation is satisfactory, and both are difficult to rationalize. The observed negative slope can only be satisfactorily explained by the possibility of a third process unaccounted for in the phase diagram, giving rise to slopes different from those predicted.

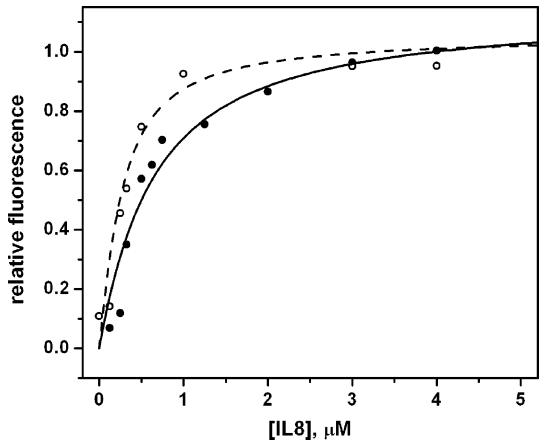

FIGURE 5: Binding of the CXCR1 N-domain to wild-type and trapped monomeric IL-8 in 3 M TMAO. The affinity of monomeric IL-8 (○) is higher than wild-type IL-8 (●), indicating that WT dimerization in 3 M TMAO is responsible for the reduced binding. The binding was measured by the change in fluorescence intensity of AlexaFluor488-labeled receptor peptide measured with excitation at 465 nm and emission at 519 nm.

What other process could be significant at high concentration regimes of IL-8 and TMAO? The answer, once arrived at, is blindingly apparent. TMAO causes proteins to fold by favoring burial of peptide groups. While the effect of TMAO on the receptor N-domain is accounted for in the phase diagram, its effect on the ligand IL-8 has been so far ignored. IL-8 monomer is highly structured and compact, and therefore TMAO is not likely to induce further structure (*17*). However, IL-8 has a propensity to dimerize, and this process involves burial of peptide groups at the dimer interface, a process that osmolytes are very likely to favor (*19*, *20*). Therefore, it is very likely that the third process in the phase diagram is in fact IL-8 dimerization and that the apparent negative dependency of IL-8 binding at higher TMAO concentrations is due to this process.

Role of Ligand Dimerization. Since TMAO favors the burying of peptide groups, it can be reasonably assumed that dimerization, which buries a significant amount of the peptide backbone, would be favored at higher TMAO concentrations. The negative slope of the phase separation line at high TMAO concentrations would be expected if dimeric IL-8 had lowered affinity to the receptor. Monomeric IL-8 has previously been shown to be sufficient for receptor binding (*11*). Further, recent studies indicate that IL-8 dimer dissociation is essential for receptor binding and that dimerization significantly reduces the affinity of IL-8 for CXCR1 (*12*; unpublished observations). If this were the case, it would explain the unexpected lower ligand affinities seen in the phase diagram at higher TMAO concentrations.

To investigate this possibility, we measured the binding of a trapped nonassociating L25NMe IL-8 monomer to the N-domain. This trapped monomer, compared to the WT, shows significantly higher affinity to the CXCR1 N-domain in 3 M TMAO (Table 1, Figure 5). Further, the observed affinity of monomeric IL-8 for the N-domain falls exactly on the predicted line (Figure 4, green triangle), confirming that dimerization is indeed the "missing link" in the linkage scheme. To further address the effect of the monomer−dimer

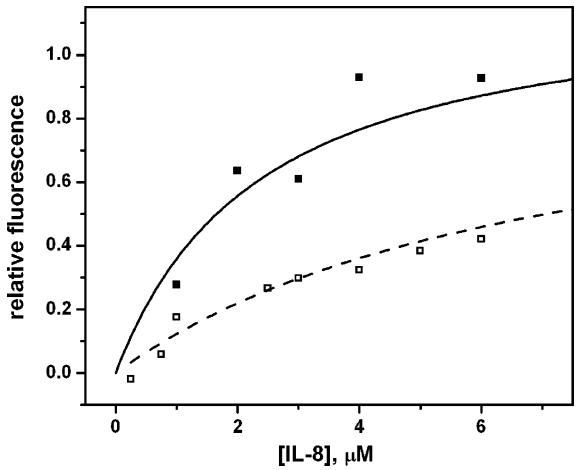

FIGURE 6: Binding of the CXCR1 N-domain to wild-type and trapped dimeric IL-8 in solution. The affinity of wild-type IL-8 (■), which is monomeric at this concentration, is significantly higher than that of trapped dimeric IL-8 (□). The binding was measured by the change in fluorescence intensity of AlexaFluor488-labeled receptor peptide measured with excitation at 465 nm and emission at 519 nm.

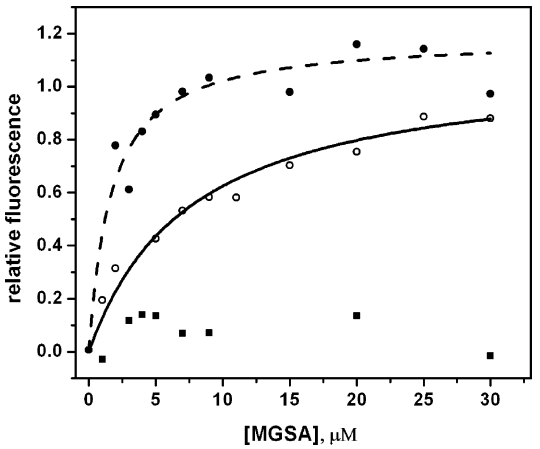

FIGURE 7: Binding of the CXCR1 N-domain to wild-type MGSA in TMAO. The affinity for MGSA increases with increasing TMAO concentrations up to 2 M [0 M TMAO (■); 0.8 M TMAO (○); 1.7 M TMAO (●)]. At TMAO concentrations higher than 2 M, binding is undetectable. The binding was measured by the change in fluorescence intensity of AlexaFluor488-labeled receptor peptide measured with excitation at 465 nm and emission at 519 nm.

equilibrium on binding affinity, we also measured the binding of a disulfide-linked trapped nondissociating R26C IL-8 dimer to the N-domain. This obligate dimer shows no detectable affinity to the N-domain in solution (Table 1, Figure 6) or in TMAO (data not shown). These observations suggest that the lowered affinities seen for WT IL-8 at high TMAO concentrations are indeed due to dimerization.

The phase diagram is therefore composed of not two but *three* coupled processes: receptor domain folding, ligand binding, and ligand dimerization, as is evident from plotting the binding affinity exhibited by the trapped L25NMe IL-8 monomer onto the phase diagram (Figure 4, green triangle). The binding affinity of the obligate monomer compared to the native protein at this TMAO concentration is significantly higher. The use of the conventional linkage scheme (Scheme 1) would not have provided insight into this three-way linkage unless one were specifically investigating such a possibility. The conventional scheme takes into account binding affinities of the unfolded and folded receptor domain and the free energy of folding. Binding affinities at different TMAO concentrations and folding energies at different ligand concentrations cannot be easily incorporated into such a format. Representation of the data graphically in the phase diagram therefore provides a simplified visual and intuitively understandable picture of such complex linkages that may not be immediately available from the conventional representation format (Scheme 1), while yet retaining or even improving the rigor of analysis of these linkages.

Role of the Receptor N-Domain in Ligand Selectivity. A characteristic feature of the chemokine/chemokine receptor system is the observation that multiple ligands bind a single receptor with similar or varying affinities. For instance, CXCR1 binds only IL-8 with high affinity and other related chemokines (such as MGSA) with low affinity (*13*, *14*). Previous structure−function studies and sequence analysis had suggested that the receptor N-domain is responsible for the differences in the observed binding affinity (*21*). We observe that MGSA does not bind to the CXCR1 N-domain in solution but binds in the presence of increasing TMAO concentrations, with affinities reaching similar to that observed for IL-8 (Table 1, Figure 7). This observation is consistent with our recent observation that the CXCR1 N-domain peptide binds both IL-8 and MGSA in micelles that mimic the native membrane environment with similar affinity (*15*). Interestingly, at higher TMAO concentrations, MGSA binding was undetectable. One interpretation of this is that the decrease in affinity due to dimerization is more pronounced in the case of MGSA than in IL-8. It is possible that dimerization of MGSA completely abrogates, instead of merely diminishing, its affinity for CXCR1. This could be looked upon as a second level of regulation of the specificity of CXCR1 for IL-8 versus MGSA. This is, however, merely speculation at this stage, and additional studies would be needed to understand the folding−binding−dimerization relationships of MGSA and CXCR1.

Structure of the N-Domain in Osmolytes, Micelles, and the Native Receptor. The currently accepted mechanisms of protein folding (such as the framework model, hydrophobic collapse, and nucleation) are essentially variations of a theme, and all propose the involvement of stabilization of secondary structural elements and compaction of the protein (*22*−*26*). The solvophobic effect of osmolytes contributes to both of these processes without significantly interfering with forces involved in native folding, such as hydrogen bonding, electrostatic, and van der Waals interactions (*3*). Studies on several soluble globular proteins have shown that osmolytes modulate native protein conformations both in vitro and in vivo inside living cells (*5*−*7*, *27*−*30*). Most interestingly, though less well studied, osmolytes have been shown to promote nativelike structure of membrane proteins in vitro in the absence of the membrane-like environment. In the only two published studies, human apolipoprotein C1 (57 residues) and the apolipoprotein AI N-domain (44 residues) were shown to adopt structures in TMAO similar to lipid-bound structures (*31*, *32*). These apolipoproteins are not embedded in the membrane but bind to the surface of lipid vesicles or detergent micelles. The CXCR1 N-domain is also not buried in the membrane in the intact receptor but is proximal to the membrane environment. The proximity of the membrane interface influences the structural and functional properties

of the N-domain, and we have shown previously that the isolated N-domain is significantly more structured and exhibits higher ligand-binding affinities in micelles (*15*). Induction of structure in the micellar or membrane environment is presumed to occur due to favorable interactions of side chains with the apolar environment of the micelle or lipid bilayer and not due to burial of the N-domain within the micelle or bilayer. The induction of secondary structure in the CXCR1 N-domain therefore occurs in the polar aqueous environment, albeit proximal to the membrane, and should follow the rules accepted for soluble proteins, with the additional factor of side-chain interaction with the micelle.

How does osmolyte-induced folding compare with that in micelles? The dominant force in osmolyte-induced folding is the unfavorable interaction of TMAO with the peptide backbone (*5*, *33*). There is little significant net interaction of osmolyte with side chains; if anything, TMAO in general exhibits a slightly favorable interaction with nonpolar side chains (*3*, *34*). Since side-chain interactions are not compromised, TMAO-induced structure is probably similar to the native N-domain structure seen in micelles and, therefore, in the native membrane environment. CD and NMR (unpublished observations) data suggest that the N-domain adopts an extended helix/turn structure in micelles, and it is very likely that the N-domain adopts a similar structure in TMAO with similar gain of function (tighter ligand binding) in both environments, with respect to both ligands. Finally, the most compelling argument in support of nativelike conformation is that it is unlikely that a non-native conformation would exhibit the observed gain of function to nativelike ligand-binding affinities, similar to those seen earlier in micelles.

Summary. We have used the protecting osmolyte TMAO to elucidate the linkage between the folded state of CXCR1 N-domain, its affinity for two different ligands, and the dimerization state of these ligands. This is the first application of osmolytes in the analysis of more than two linked biological processes. The use of the phase diagram to represent our data has made it possible to visualize the complex thermodynamic linkages among different interactions that have very similar equilibrium constants. On a general level, our studies demonstrate the use of osmolytes and phase diagrams in the analysis of complex thermodynamically linked biological processes. N-Terminal domains of chemokine receptors CXCR3, CCR3, CCR5, and CX3CR1 have also been shown to bind their cognate ligands in solution using a variety of techniques including surface plasmon resonance, fluorescence, competition binding, and NMR (*11*, *14*, *35*−*39*). The measured binding affinities are weak and can be attributed to the fact that the receptor N-domains peptides are unstructured, and it is very likely that tighter and more nativelike binding will be observed if measured in the presence of osmolytes.

Our studies also indicate a possible regulatory role for chemokine dimerization in receptor-binding affinity. We observe that dimerization reduces the affinity of IL-8 for its receptor CXCR1, in concordance with earlier observations by our group (*12*). We also observe that dimerization has different apparent effects on binding affinity in the case of two different ligands, indicating that dimerization of different ligands could differentially regulate their binding affinities to the same receptor. Structure determination and solution characterization indicate that many chemokines dimerize, and our study emphasizes the importance of measuring binding under conditions where the ligand is monomeric and/or using a mutant monomeric chemokine such as the trapped L25NMe IL-8 monomer used in this study.

ACKNOWLEDGMENT

We thank Dr. Jim Lee and Ms. Lucy Lee for helpful discussions, technical advice, and assistance with CD measurements. We also thank Dr. Kurosky, Mr. Steve Serabyn, and Mr. Phil Owen for help with peptide synthesis.

REFERENCES

1. Hochachka, P. W., and Somero, G. N. (2002) *Biochemical Adaptation*, Oxford University Press, Oxford.
2. Yancey, P. H., Clark, M. E., Hand, S. C., Bowlus, R. D., and Somero, G. N. (1982) Living with water stress: evolution of osmolyte systems, *Science 217*, 1214−1222.
3. Bolen, D. W., and Baskakov, I. V. (2001) The osmophobic effect: natural selection of a thermodynamic force in protein folding, *J. Mol. Biol. 310*, 955−963.
4. Dedmon, M. N., Patel, C. N., Young, G. B., and Pielak, G. J. (2002) FlgM gains structure in living cells, *Proc. Natl. Acad. Sci. U.S.A. 99*, 12681−12684.
5. Baskakov, I., and Bolen, D. W. (1998) Forcing thermodynamically unfolded proteins to fold, *J. Biol. Chem. 273*, 4831−4834.
6. Henkels, C. H., Kurz, J. C., Fierke, C. A., and Oas, T. G. (2001) Linked folding and anion binding of the *Bacillus subtilis* ribonuclease P protein, *Biochemistry 40*, 2777−2789.
7. Kumar, R., Lee, J. C., Bolen, D. W., and Thompson, E. B. (2001) The conformation of the glucocorticoid receptor af1/tau1 domain induced by osmolyte binds co-regulatory proteins, *J. Biol. Chem. 276*, 18146−18152.
8. Luster, A. D. (2002) The role of chemokines in linking innate and adaptive immunity, *Curr. Opin. Immunol. 14*, 129−135.
9. Clore, G. M., Appella, E., Yamada, M., Matsushima, K., and Gronenborn, A. M. (1990) Three-dimensional structure of interleukin 8 in solution, *Biochemistry 29*, 1689−1696.
10. Baldwin, E. T., Weber, I. T., St. Charles, R., Xuan, J. C., Appella, E., Yamada, M., Matsushima, K., Edwards, B. F., Clore, G. M., Gronenborn, A. M., and Wlodawer, A. (1991) Crystal structure of interleukin 8: symbiosis of NMR and crystallography, *Proc. Natl. Acad. Sci. U.S.A. 88*, 502−506.
11. Rajarathnam, K., Sykes, B. D., Kay, C. M., Dewald, B., Geiser, T., Baggiolini, M., and Clark-Lewis, I. (1994) Neutrophil activation by monomeric interleukin-8, *Science 264*, 90−92.
12. Fernando, H., Chin, C., Rösgen, J., and Rajarathnam, K. (2004) Dimer dissociation is essential for interleukin-8 (IL-8) binding to CXCR1 receptor, *J. Biol. Chem. 279*, 36175−36178.
13. Jones, S. A., Dewald, B., Clark-Lewis, I., and Baggiolini, M. (1997) Chemokine antagonists that discriminate between interleukin-8 receptors. Selective blockers of CXCR2, *J. Biol. Chem. 272*, 16166−16169.
14. Lowman, H. B., Slagle, P. H., DeForge, L. E., Wirth, C. M., Gillece-Castro, B. L., Bourell, J. H., and Fairbrother, W. J. (1996) Exchanging interleukin-8 and melanoma growth-stimulating activity receptor binding specificities, *J. Biol. Chem. 271*, 14344−14352.
15. Rajagopalan, L., and Rajarathnam, K. (2004) Ligand selectivity and affinity of chemokine receptor CXCR1: Role of N-terminal domain, *J. Biol. Chem. 279*, 30000−30008.
16. Rösgen, J., and Hinz, H.-J. (2003) Phase diagrams: a graphical representation of linkage relations, *J. Mol. Biol. 328*, 255−271.
17. Rajarathnam, K., Clark-Lewis, I., and Sykes, B. D. (1995) ^{1}H NMR Solution structure of an active interleukin-8 monomer, *Biochemistry 34*, 12983−12990.
18. Santoro, M. M., and Bolen, D. W. (1988) Unfolding free energy changes determined by the linear extrapolation method. 1. Unfolding of phenylmethanesulfonyl alpha-chymotrypsin using different denaturants, *Biochemistry 27*, 8063−8068.

19. Patel, C. N., Noble, S. M., Weatherly, G. T., Tripathy, A., Winzor, D. J., and Pielak, G. J. (2002) Effects of molecular crowding by saccharides on alpha-chymotrypsin dimerization, *Protein Sci. 11*, 997−1003.
20. Shearwin, K. E., and Winzor, D. J. (1988) Effect of sucrose on the dimerization of alpha-chymotrypsin. Allowance for thermodynamic nonideality arising from the presence of a small inert solute, *Biophys. Chem. 31*, 287−294.
21. Gayle, R. B., Sleath, P. R., Srinivason, S., Birks, C. W., Weerawarna, K. S., Cerretti, D. P., Kozlosky, C. J., Nelson, N., Bos, T. V., and Beckmann, M. P. (1993) Importance of the amino terminus of the interleukin-8 receptor in ligand interactions. *J. Biol. Chem. 268*, 7283−7289.
22. Wetlaufer, D. B. (1973) Nucleation, rapid folding, and globular intrachain regions in proteins, *Proc. Natl. Acad. Sci. U.S.A. 70*, 697−701.
23. Ptitsyn, O. B. (1987) Protein folding: hypotheses and experiments, *J. Protein Chem. 6*, 273−329.
24. Lindorff-Larsen, K., Rogen, P., Paci, E., Vendruscolo, M., and Dobson, C. M. (2005) Protein folding and the organization of the protein topology universe, *Trends Biochem. Sci. 30*, 13−19.
25. Baldwin, R. L. (1989) How does protein folding get started?, *Trends Biochem. Sci. 14*, 291−294.
26. Daggett, V., and Fersht, A. R. (2003) Is there a unifying mechanism for protein folding?, *Trends Biochem. Sci. 28*, 18−25.
27. Uversky, V. N., Li, J., and Fink, A. L. (2001) Trimethylamine-*N*-oxide-induced folding of alpha-synuclein, *FEBS Lett. 509*, 31−35.
28. Welch, W. J., and Brown, C. R. (1996) Influence of molecular and chemical chaperones on protein folding, *Cell Stress Chaperones 1*, 109−115.
29. Brown, C. R., Hong-Brown, L. Q., and Welch, W. J. (1997) Correcting temperature-sensitive protein folding defects, *J. Clin. Invest. 99*, 1432−1444.
30. Ignatova, Z., and Gierasch, L. M. (2004) Monitoring protein stability and aggregation in vivo by real-time fluorescent labeling, *Proc. Natl. Acad. Sci. U.S.A. 101*, 523−528.
31. Gursky, O. (1999) Probing the conformation of a human apolipoprotein C-1 by amino acid substitutions and trimethylamine-*N*-oxide, *Protein Sci. 8*, 2055−2064.
32. Zhu, H. L., and Atkinson, D. (2004) Conformation and lipid binding of the N-terminal (1−44) domain of human apolipoprotein A-I, *Biochemistry 43*, 13156−13164.
33. Wang, A., and Bolen, D. W. (1997) A naturally occurring protective system in urea-rich cells: mechanism of osmolyte protection of proteins against urea denaturation, *Biochemistry 36*, 9101−9108.
34. Zou, Q., Bennion, B. J., Daggett, V., and Murphy, K. P. (2002) The molecular mechanism of stabilization of proteins by TMAO and its ability to counteract the effects of urea, *J. Am. Chem. Soc. 124*, 1192−1202.
35. Ye, J., Kohli, L. L., and Stone, M. J. (2000) Characterization of binding between the chemokine eotaxin and peptides derived from the chemokine receptor CCR3, *J. Biol. Chem. 275*, 27250−27257.
36. Mayer, K. L., and Stone, M. J. (2000) NMR solution structure and receptor peptide binding of the CC chemokine eotaxin-2, *Biochemistry 39*, 8382−8395.
37. Farzan, M., Chung, S., Li, W., Vasilieva, N., Wright, P. L., Schnitzler, C. E., Marchione, R. J., Gerard, C., Gerard, N. P., Sodroski, J., and Choe, H. (2002) Tyrosine-sulfated peptides functionally reconstitute a CCR5 variant lacking a critical amino-terminal region, *J. Biol. Chem. 277*, 40397−40402.
38. Mizoue, L. S., Bazan, J. F., Johnson, E. C., and Handel, T. M. (1999) Solution structure and dynamics of the CX3C chemokine domain of fractalkine and its interaction with an N-terminal fragment of CX3CR1, *Biochemistry 38*, 1402−1414.
39. Booth, V., Keizer, D. W., Kamphuis, M. B., Clark-Lewis, I., and Sykes, B. D. (2002) The CXCR3 binding chemokine IP-10/CXCL10: Structure and receptor interactions, *Biochemistry 41*, 10418−10425.

BI051219Z